Hagen, D. J.; Mai, L.; Devi, A.; Sainio, J.; Karppinen, M.

# Atomic/molecular layer deposition of Cu-organic thin films

*Published in:*
Dalton Transactions

*DOI:*
10.1039/C8DT03735C

Published: 01/01/2018

*Document Version*
Peer-reviewed accepted author manuscript, also known as Final accepted manuscript or Post-print

*Published under the following license:*
Unspecified

*Please cite the original version:*
Hagen, D. J., Mai, L., Devi, A., Sainio, J., & Karppinen, M. (2018). Atomic/molecular layer deposition of Cu-organic thin films. *Dalton Transactions*, *47*(44), 15791-15800. https://doi.org/10.1039/C8DT03735C

Journal Name

ARTICLE

# Atomic/molecular layer deposition of Cu-organic thin films

D. J. Hagen,[a] L. Mai,[b] A. Devi,[b] J. Sainio,[c] and M. Karppinen[a*]

Received 00th January 20xx,
Accepted 00th January 20xx

DOI: 10.1039/x0xx00000x

www.rsc.org/

The gas-phase atomic/molecular layer deposition (ALD/MLD) technique is strongly emerging as a viable approach to fabricate new exciting inorganic-organic hybrid thin-film materials. However, there have been much less efforts to develop new precursors specifically intended for ALD/MLD; this applies to both the organic and inorganic precursors, and in the latter case in particularly to the transition metal precursors. Here we introduce copper bisdimethylaminopropoxide ($Cu(dmap)_2$) as a promising transition metal precursor for ALD/MLD to be combined with a variety of organic precursors with different backbones and functional groups, i.e. hydroquinone (HQ), terephthalic acid (TPA), 4,4'-oxydianiline (ODA), p-phenylenediamine (PPDA) and 1,4-benzendithiol (BDT). Hybrid Cu-organic thin films were obtained from all the five organic precursors with appreciably high growth rates ranging from 1.0 to 2.6 Å/cycle. However, the $Cu(dmap)_2$+HQ process was found to yield hybrid Cu-organic films only at temperatures below 120 °C, while at the higher temperatures metallic Cu films were obtained. The films were characterized by XRR, GIXRD, FTIR, Raman, XPS and UV-Vis spectroscopy.

## Introduction

Hybrid inorganic-organic materials may – once smartly built up – offer exciting synergistic properties unattainable with the conventional materials; they could for example bring together mechanical flexibility typical for organic polymers and various functionalities derived from the partly filled d orbitals of transition metals such as electrical conductivity, magnetism or catalytic activity. A major part of the vast research carried out in the field concerns bulk materials; to widen the application window progress in the thin-film fabrication of these materials is required too.[1,2]

For the fabrication of well-defined hybrid thin films, the state-of-the-art atomic/molecular layer deposition (ALD/MLD) technique based on gaseous (thermally evaporated/sublimated) precursors is currently strongly emerging as an exciting new approach.[3-5] The parent ALD technique has already since several decades earned its position as a leading technology for the fabrication of high-quality inorganic thin films in microelectronics industry,[6] while its analogue in the case of purely organic thin films, i.e. MLD,[7] has been much less exploited so far. For the fabrication of hybrid inorganic-organic thin films, ALD cycles are combined with MLD cycles by pulsing the metal and organic precursors into the reactor in a sequential manner. This enables the layer-by-layer deposition of inorganic-organic thin films with an atomic/molecular level precision and the desired intimate interaction between the metal cations and the organic moieties. Through ALD/MLD different types of new hybrid thin-film materials have already been realized, with exciting barrier,[8,9] optical,[10] luminescence,[11-15] thermoelectric,[16,17] battery[18] and metal-organic framework[19-24] application-relevant properties.

Like in ALD and MLD, also in ALD/MLD the prototype processes are based on ligand-exchange gas-surface reactions. For such reactions the metal precursor should possess two ligands in minimum and the organic precursor two functional groups in minimum; this stems from the continuity requirement of the surface reactions upon the repetition of the deposition cycles. A common example of such ALD/MLD processes is the reaction between $Zn(C_2H_5)_2$ and diethylene glycol precursors.[25] The process yields hybrid zinc ethanediolate $[ZnO(C_2H_4)O]_n$ thin films as intended but an obvious issue with this and similar processes based on organic precursors with readily bendable alkyl-chain backbones is the high probability of unwanted double reactions of the organic precursor on the film surface, leading to a gradually declining film growth.[4,26] The more rigid organic molecules based on e.g. benzene ring(s), such as hydroquinone and 4,4'-oxydianiline, are believed not to suffer from this problem.[27,28] Heterofunctional organic precursors could be another solution to avoid the unwanted double reactions, as dissimilar functional groups most likely react differently with the metal-ligand surface sites; an example is 4-aminophenol (AP) with both OH and $NH_2$ groups.[29,30] A number of ALD/MLD processes have indeed been developed based on the aforementioned aromatic organic precursors; in most cases however the metal component (e.g. $Al^{3+}$, $Zn^{2+}$, or $Ti^{4+}$) has lacked the partly filled d-orbitals.

The ALD/MLD growth of hybrid thin films containing middle to late transition metal species has been little challenged, in part owing to the lack of suitable precursors for these metals. For example, alkyl organometallics of transition metals are typically unstable. In ALD, β-diketonate complexes are often used as transition metal precursors, but due to their limited reactivity the processes typically require ozone as the second reactant.[31-33] Most of the organic precursors are not reactive enough to be combined with the metal diketonate precursors for effective ALD/MLD processes. However, we recently demonstrated that terephthalic acid and its derivatives readily form hybrids with diketonates of most transition metals including Cu, Co and Mn,[18,34] and also of the main-group metals.[19,21,35]

To be able to extend the ALD/MLD technique to a wider range of transition-metal components, it is crucially important to search for

[a] Department of Chemistry and Materials Science, Aalto University, Espoo, Finland.
[b] Department of Chemistry, Ruhr University, Bochum, Germany.
[c] Department of Applied Physics, Aalto University, Espoo, Finland.
* email: maarit.karppinen@aalto.fi

alternative precursors that are more reactive than the diketonate complexes. Such a work is certainly going on but the new precursors containing these elements are usually investigated only for their use in ALD, especially for the deposition of elemental metals.[36-43] In particular, Cu-bisdimethylaminopropoxide or $Cu(dmap)_2$ appears to be a promising new precursor candidate: it is at the same time sufficiently reactive, as it has been successfully used for the thermal ALD of Cu,[36,44,45] $Cu_2O$[46] and $Cu_3N$[47] at low temperatures, but stable enough as judged by its low sublimation temperature (~60 °C) and relatively high decomposition temperature (>200 °C). The low sublimation temperature moreover allows the low-temperature depositions required in the case of sensitive substrate materials.[48]

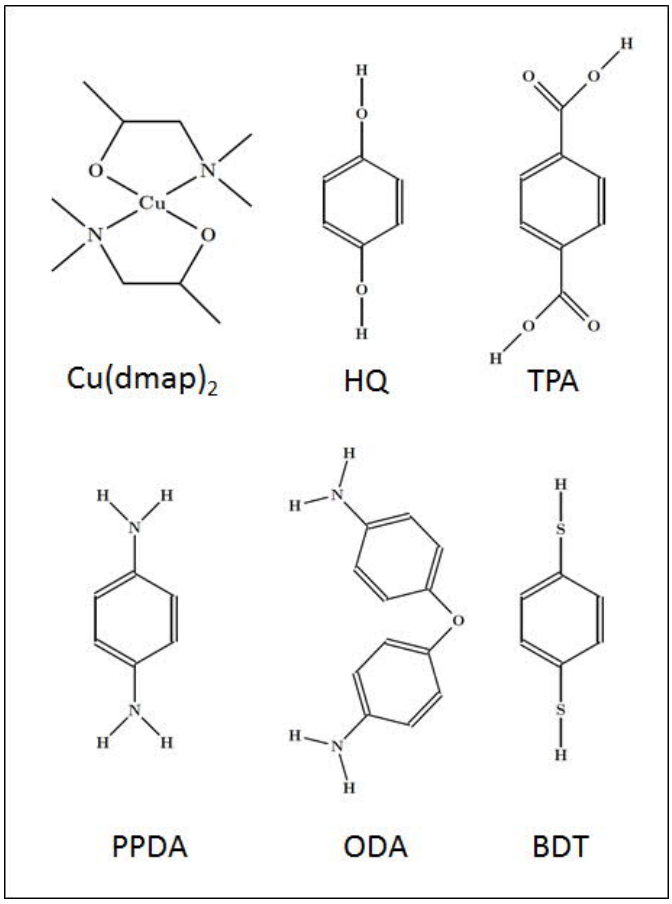


**Fig. 1** Molecular structures of the precursors used in this work.

In this work, we explore $Cu(dmap)_2$ as a precursor for the use in ALD/MLD of hybrid thin films in combination with a variety of organic precursors, , i.e. hydroquinone (HQ), terephthalic acid (TPA), 4,4'-oxydianiline (ODA), p-phenylenediamine (PPDA) and benzene-1,4,-dithiol (BDT), see Fig. 1. The first two organic precursors were chosen based on the facts that so far HQ has been the most common aromatic precursor used in ALD/MLD processes, and TPA the only organic precursor for which the ALD/MLD of Cu-organic thin films has been successfully demonstrated. It should be noted that we used HQ in our earlier works in combination with copper bisacetylacetonate or $Cu(acac)_2$, but this process yielded metallic Cu films rather than hybrid ones. However, here the high vapour pressure of $Cu(dmap)_2$ allows the use of lower deposition temperatures which could promote the hybrid formation. Then, we also find the amino groups interesting to be investigated in combination with $Cu(dmap)_2$ as they are typically less reactive in MLD processes than the hydroxyl groups.[29,49] However, amino groups have been shown to react with many metal precursors, as was shown for the amino groups of ODA in combination with $TiCl_4$.[28] Hence, it is interesting to investigate the deposition of late-transition-metal hybrids using organic precursors with amino groups as such attempts have not been reported thus far. In particular, the simplest amide PPDA has not been challenged in any ALD/MLD process at all. Finally, we also evaluate the thiol precursor BDT for the first time.

## Experimental Methods

All the Cu-organic thin-film depositions were carried out using an ASM Microchemistry F-120 reactor. The copper precursor $Cu(dmap)_2$ was prepared according to literature methods,[50] and the organic compounds were purchased (Sigma Aldrich, Alfa Aesar). The precursors were placed in open boats inside the reactor and $N_2$ was used as a carrier and purging gas. Substrates were Si (100) and boro-silicate glass, which were degreased with ethanol before the deposition. In Table 1, the deposition parameters are given for all the five ALD/MLD processes investigated.

**Table 1** Deposition parameters used in the six new ALD/MLD processes developed in this work. The sublimation temperature and pulse/purge times for $Cu(dmap)_2$ were 60 °C and 7 s/5 s. For ODA and PPDA, the third values for the deposition temperature and the corresponding number of cycles values refer to the experiments in which these values were kept constant.

| Org. prec. | Subl. temp. (°C) | Pulse/purge times (s) | Dep. temp. (°C) | No. of cycles |
|---|---|---|---|---|
| HQ | 100 | 8/10 | 100–180 | 600 |
| TPA | 160 | 10/10 | 160 | 600 |
| ODA | 140 | 8/10 | 140–240, 160 | 50–750, 450 |
| PPDA | 70 | 8/10 | 70–240, 100 | 50–1000, 600 |
| BDT | 35 | 10/10 | 80–149 | 700 |

The film thicknesses were determined by X-ray reflection (XXR) using a Panalytical XPert diffractometer equipped with a Cu $K_\alpha$ source. The same tool was used to investigate the degree of crystallinity by grazing incidence X-ray diffraction (GIXRD) using an incidence angle of 0.5°. The film morphologies were evaluated by atomic force microscopy (AFM) with a D5000 Nanoscope 5 operated in tapping mode. Fourier-transformation infrared spectroscopy (FTIR) was conducted with a Nicolet Protégé 460 spectrometer and UV/vis spectroscopy with a Perkin Elmer Lambda 2 spectrometer. Raman spectra were measured with a Horiba Jobin-Yvon Labram HR Raman spectrometer for the Cu-TPA and Cu-BDT films using an Ar-ion-laser with a wavelength of 514 nm as the light source and for the Cu-ODA and Cu-PPDA films using a semiconductor laser with a wavelength of 785 nm. X-ray photoelectron spectroscopy (XPS) was performed with a Kratos Axis Ultra spectrometer using monochromated Al $K_\alpha$ radiation and charge neutralization. The spectra were acquired using a pass energy of 80 eV, an X-ray power between 100 and 225 W and an analysis spot of roughly 200 µm in diameter.

## Results and Discussion

**Film growth.** We first carried out preliminary depositions with all the organic precursors to evaluate their reactivities with $Cu(dmap)_2$ and to investigate the resultant film compositions.; Table 2 summarizes the results of these experiments. For all the five organic precursors, conditions were found so that the processes yielded hybrid thin films.

In the case of HQ as the organic precursor, it was interesting to observe the effect of the deposition temperature: at the higher deposition temperatures the $Cu(dmap)_2$+HQ process yielded metallic Cu films like in our previous study with $Cu(acac)_2$ as the copper precursor.[51] However, the low sublimation temperature of $Cu(dmap)_2$ allowed us to carry out depositions also in the lower temperature range of 100–120 °C where amorphous Cu-organic films were obtained. With ODA, amorphous hybrid films were obtained at deposition temperatures up to ~220 °C, whereas at 240 °C the $Cu(dmap)_2$+ODA process too yielded metallic Cu films. Note that even at 220 °C, a weak Cu signal was seen, though. The formation of Cu is due to the decomposition of $Cu(dmap)_2$ above 200 °C.[48]

**Table 2** Summary of the results from the deposition experiments together with relevant results from our previous works: film growth rate (i.e. growth-per-cycle, GPC) and the resultant composition of the thin films (i.e. metallic Cu film or hybrid Cu-organic film).

| Copper prec. | Org. prec. | Dep. T (°C) | GPC (Å/c) | Mater. | Ref. |
|---|---|---|---|---|---|
| $Cu(acac)_2$ | HQ | 180–280 | 2.0 | Cu | [18] |
| $Cu(dmap)_2$ | HQ | 100–120 | 1.0–1.5 | hybrid | present |
| $Cu(dmap)_2$ | HQ | 140–180 | 0.3 | Cu | present |
| $Cu(thd)_2$ | TPA | 180–220 | 3.0–0.7 | hybrid | [51] |
| $Cu(dmap)_2$ | TPA | 160 | 2.6 | hybrid | present |
| $Cu(dmap)_2$ | ODA | 140–220 | 2.4 | hybrid | present |
| $Cu(dmap)_2$ | ODA | 240 | 1.5 | Cu | present |
| $Cu(dmap)_2$ | PPDA | 70–200 | 1.7 | hybrid | present |
| $Cu(dmap)_2$ | BDT | 80–140 | 1.9–0.8 | hybrid | present |

In Table 2 we summarize the (average) growth-per-cycle (GPC) values determined for the different processes. For all the hybrid processes, the GPC values are within 0.8 and 2.6 Å/cycle. The highest GPC value of 2.6 Å/cycle was achieved with TPA at 160 °C; this value is very similar to the GPC values previously obtained for the $Cu(thd)_2$+TPA process at the lowest deposition temperatures.[18] These high GPC values can be explained with the high acidity and thus reactivity of the carboxyl group. With ODA, a slightly lower GPC value of 2.4 Å/cycle was obtained; ODA contains much less acidic amino groups, but the backbone of the ODA molecule is bulkier explaining the yet relatively high GPC value. In line with this, clearly lower GPC values of 1.7 and 1.9 Å/cycle were obtained with PPDA, which could be explained with the smaller sizes of these molecules as compared to ODA. Slightly lower GPC values of 1.0–1.5 Å/cycle were measured for the hybrid film growth with HQ at 120 °C. With BDT, the GPC value seemed to decrease with deposition temperature, from 1.9 Å/cycle at 80 °C to 0.8 Å/cycle at 140 °C. However, the sublimation temperature of BDT is only 35 °C, thus close to room temperature, which made it difficult to use it in the open boat configuration of our F-120 reactor, and hence some parasitic effects could not be ruled out.

Finally, we discuss the growth rates for the processes yielding metallic copper films. For the $Cu(dmap)_2$+HQ process at temperatures above 120 °C the GPC was quite low (0.3 Å/cycle) which is a typical value for copper ALD processes based on Cu(II)-aminoalkoxides as the copper source.[43,44] This confirms the reductive behaviour of HQ observed in our earlier work.[51] On the other hand, the much higher GPC value of 1.5 Å/cycle for the $Cu(dmap)_2$+ODA process at 240 °C is typical for a CVD-type growth of copper films.

**Deposition parameters.** We selected the $Cu(dmap)_2$+ODA and $Cu(dmap)_2$+PPDA processes for a more detailed process parameter investigation. These two organic precursors were chosen as they have wider potential temperature windows than e.g. HQ and TPA (as with HQ the depositions resulted in the formation of metallic Cu at a temperature as low as 140 °C, and with TPA the high sublimation temperature is quite close to the onset of the decomposition of $Cu(dmap)_2$).

The two processes, $Cu(dmap)_2$+ODA and $Cu(dmap)_2$+PPDA, were investigated in the temperature ranges of 140–240 °C and 70–240 °C, respectively, see Fig. 2(a); for the former process the low-temperature end was determined by the sublimation temperature of ODA, while for the latter process the smaller size of the PPDA molecule and its accordingly higher vapour pressure and lower sublimation temperature allowed the deposition experiments starting from temperatures as low as 70 °C. The precursor pulsing sequence for both processes was: 7 s $Cu(dmap)_2$, 5 s $N_2$ purge, 8 s organic precursor, 10 s $N_2$ purge. From Fig. 2(a), the GPC remains nearly constant for both processes (at ~2.3 and ~1.6 Å/cycle) up to 200–220 °C, then significantly decreases at 240 °C. This decrease is most likely due to a decomposition of the films, which is also suggested by their degraded visual appearances. These results suggest ALD windows ranging from the sublimation temperatures to the decomnposition onset of $Cu(dmap)_2$ for both processes.

The saturation of the surface reactions was confirmed at 160 °C for the $Cu(dmap)_2$+ODA process by varying the pulse lengths of the two precursors one at the time, while for the $Cu(dmap)_2$+PPDA process the saturation experiments were carried out at 100 °C; note that in the latter case we only varied the pulse length of PPDA as the deposition temperature for this process is typical for the $Cu(dmap)_2$ ALD processes where this Cu precursor is known to reach surface with relatively short pulse lengths. As can be seen from 2(b), the GPC value saturates quite well for both the processes when the $Cu(dmap)_2$ pulse length exceeds 4 s and the organic precursor length exceeds 3 s for ODA and 4s for PPDA. Note that in the case of the $Cu(dmap)_2$+ODA process the data are somewhat more scattered, which is not surprising giving the large size of the ODA moiety.

Finally, we plot in Fig. 2(c) the film thickness against the number of ALD/MLD cycles. For the $Cu(dmap)_2$+PPDA process, the film thickness linearly increases with increasing number of deposition cycles as expected for an ideal ALD/MLD process. For the $Cu(dmap)_2$+ODA process, on the other hand, a weakly declining trend is seen. Similar observations have been made for several MLD and ALD/MLD processes, presumably due to concurrent single and double surface reactions of the organic molecule. For the ODA molecule due to its angled ether bond the unwanted double surface reactions where the ODA molecule reacts with the surface sites via both of its functional amino groups are sterically possible.

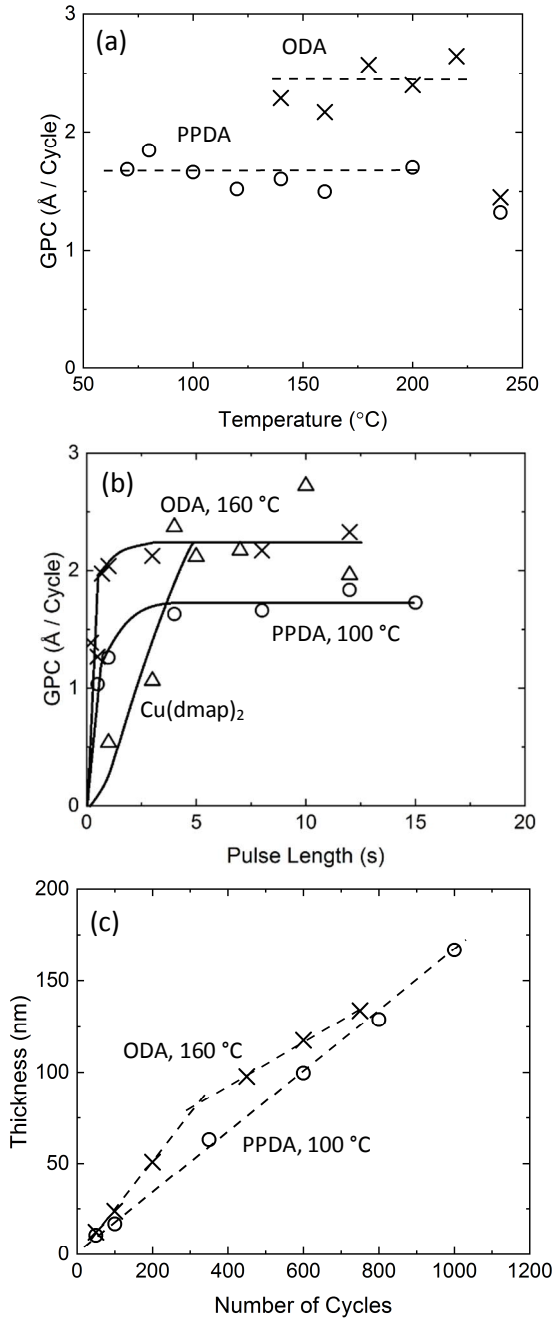


**Fig. 2** Optimization of the $Cu(dmap)_2$+ODA (o) and $Cu(dmap)_2$+PPDA (x) process parameters on Si: (a) GPC versus deposition temperature; (b) GPC versus precursor pulse lengths, triangles are for the $Cu(dmap)_2$ pulse; (c) film thickness versus number of ALD/MLD cycles. In (b) and (c), the deposition temperature was 160 °C for the $Cu(dmap)_2$+ODA process, and 100 °C for the $Cu(dmap)_2$+PPDA process.

**Crystallinity and stability.** All our as-deposited Cu-organic hybrid thin films were amorphous or nanocrystalline from GIXRD data. Fig. 3 shows representative GIXRD patterns for the Cu-PPDA, Cu-ODA and Cu-HQ films. For Cu-ODA, no sign of crystallinity could be observed in any of the as-deposited films, except for metallic Cu in the case of the depositions carried out above 200 °C (not shown). Amorphous films were also obtained for the Cu-BDT and Cu-TPA films. Note that the latter observation is in contrast to our earlier work where $Cu(thd)_2$ was used as the copper precursor, as this processes was found to yield crystalline hybrid films in the temperature range 180–190 °C.[18] From Fig. 3, the diffraction pattern for the Cu-PPDA film deposited with 1000 cycles at 100 °C shows a broad peak between 22 and 31 ° suggesting a certain degree of nanocrystallinity. The most interesting observations were made for the Cu-HQ films. The as-deposited film at 120 °C consists of an amorphous hybrid phase and some metallic Cu. The hybrid film was evident from visual inspection and FTIR analysis discussed below. Upon an exposure to air for about two days the colour of the film changed and it became coarse, while the GIXRD revealed the appearance of a new set of low-angle peaks below 20 ° indicating a new crystalline hybrid phase.

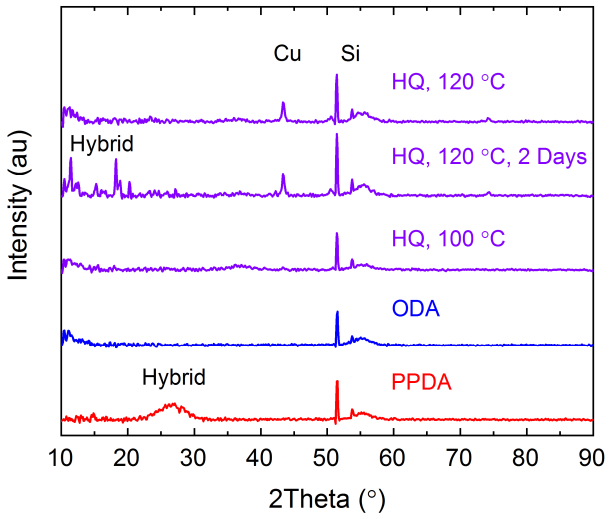


**Fig. 3** Representative GIXRD patterns for films deposited with the $Cu(dmap)_2$ and PDDA (100 °C, 1000 cycles) or ODA (160 °C, 750 cycles), and patterns for two films deposited with HQ at 120 °C: as-deposited and air-stored for 2 days.

The as-deposited films were quite smooth. In Fig. 4 we show as an example an AFM image for a representative Cu-ODA film deposited with 450 cycles at 180 °C. The RMS roughness value is clearly below 1 nm and no sign of porosity is seen. Similar observations were also made for the other amorphous hybrid films.

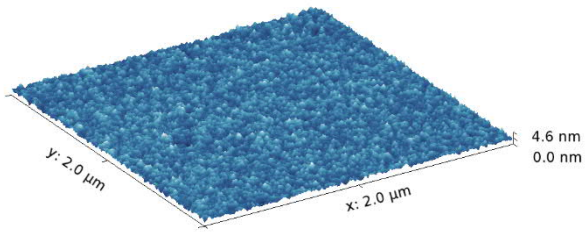


**Fig. 4** AFM image for a Cu-ODA film deposited at 180 °C.

Judging from visual inspection, the Cu-TPA and the Cu-ODA films were quite air-stable, which was surprising to us given the air-sensitivity usually observed e.g. for Cu-amides.[41] The Cu-PPDA films were stable enough to be characterized after air-exposure, although they appeared to be slightly more air-sensitive than the Cu-ODA films.

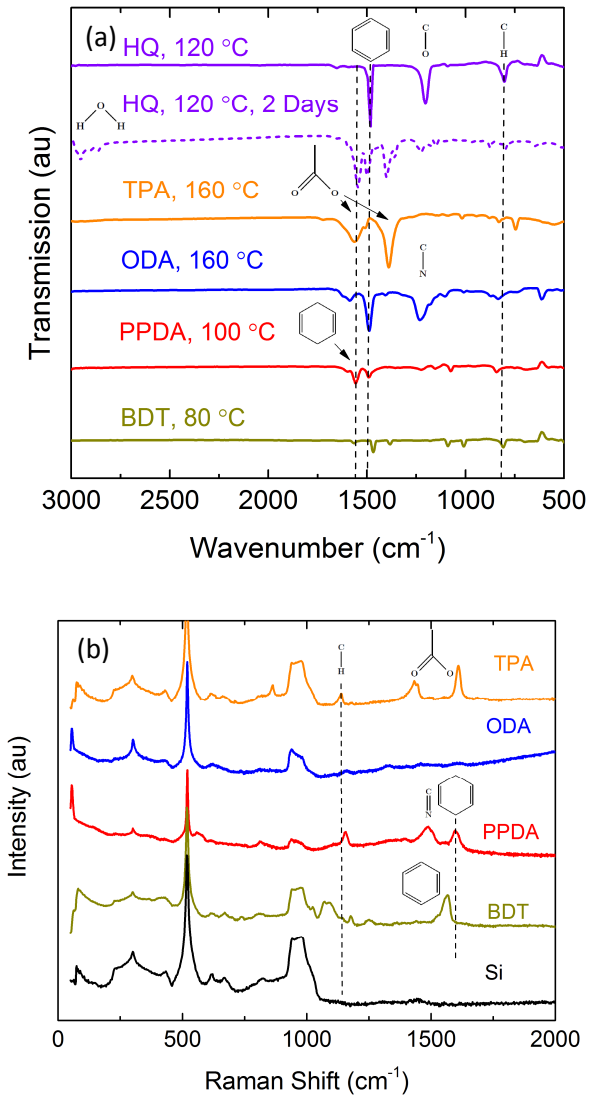


**Fig. 5** (a) FTIR and (b) Raman spectra for representative hybrid films deposited with $Cu(dmap)_2$ and the different organic precursors; the FTIR spectra are transmission spectra after subtraction of the Si spectrum.

**Bonding characteristics.** We investigated the organic moieties and the type of bonding in our hybrid thin films with FTIR, Raman and XPS experiments. Firstly, for all the hybrid films except the Cu-PPDA films the presence of benzene rings could be readily confirmed from the FTIR spectra, see Fig. 5(a). These features (near 1500 $cm^{-1}$) due to aromatic rings were clearly seen – among others – for the films yielded from the $Cu(dmap)_2$+HQ process at deposition temperatures below 120 °C, but not for the films deposited at 140 °C or higher being composed of metallic Cu according to the GIXRD data. Additionally, the peak at 1205 $cm^{-1}$ arises from the C-O vibration and that at 802 $cm^{-1}$ originates from the C-H vibrations.[52] Interestingly, when the Cu-HQ film upon the air-storage became crystalline (and lost its blue colour and became very coarse) new broad absorption peaks appeared in the FTIR spectrum between 2820 and 3030 $cm^{-1}$ (Fig. 5(a)), which is typical of water. Since the features due to the aromatic ring and the C-O bond remained essentially intact, our tentative conclusion is that the absorbed water is coordinated to the metal centre, thereby promoting the crystallization of the hybrid material.

For the carboxylates, the FTIR spectrum reveals information of the coordination type of the carboxyl groups, because the separation between the symmetric and asymmetric O-C-O vibrations differs significantly between the bidentate, monodentate and bridging coordination.[53] For the Cu-TPA film the FTIR spectrum clearly indicates that the carboxyl groups are bonded in the bridging-type mode based on the difference of 174 $cm^{-1}$ between the symmetric and asymmetric vibrations at 1390 and 1564 $cm^{-1}$. Thus the bonding structure is very similar to that previously seen for the Cu-TPA films grown from $Cu(acac)_2$.[18]

Likewise, the FTIR spectrum of the Cu-ODA film is quite similar to the spectrum previously obtained for a Ti-ODA film.[28] The features at 1490, 1315 and 1230 $cm^{-1}$ correspond to the C-C stretching within the aromatic ring, the C-O-C bond and the C-N bond, respectively,[28] while the one at 1590 $cm^{-1}$ results from H-N-H shearing. The latter absorption is quite weak; hence we may conclude that – similarly to the $TiCl_4$+ODA process – in the $Cu(dmap)_2$+ODA process too both the H atoms from each ODA amine group react with $Cu(dmap)_2$ and only the surface amine groups from the last ODA pulse are left intact in the resultant thin film. In the Cu-PPDA spectrum, on the other hand, the absorption due to the C-C stretching of the aromatic ring at 1490 $cm^{-1}$ is much weaker and virtually no C-N peak around 1240 $cm^{-1}$ can be detected. At the same time, there is an additional peak at 1557 $cm^{-1}$, which most likely could be due to quinoid-type C-C vibration.[54] Note that a quinoid ring would be expected from the formation of imino groups.

Unfortunately, for the Cu-BDT film the FTIR spectrum is quite weak; nevertheless the peaks seen at 1466, 1385 and 1009 $cm^{-1}$ most likely originate from the aromatic ring,[55,56] thus confirming the hybrid composition.

Raman spectroscopy often provides complementary information to the information obtained by FTIR. Therefore, we collected Raman spectra for our hybrid thin films, see Fig. 5(b). An illustrative example of the complementarity of the two techniques is the Cu-PPDA films: while the FTIR spectrum was very weak, the Stokes lines are clearly visible with peaks at 558, 1155, 1485 and 1603 $cm^{-1}$. These lines can be interpreted as resulting from out-of-plane ring deformation, C-H bending, the C=N stretching, and the C=C stretching of the quinoid ring, respectively.[57] Thus, the Raman spectrum confirms our tentative conclusion based on the FTIR data for Cu-PPDA.

Similarly, valuable information can be revealed with Raman spectroscopy for Cu-BDT for which Stokes lines are seen at 365, 414, 736, 1024, 1074, 1176, 1253 and 1566 $cm^{-1}$. Most of these lines originate from the benzene ring. The small peak at 2527 $cm^{-1}$ is due to unreacted SH groups, presumably at the film surface.

The Raman spectrum of Cu-TPA is dominated by peaks at 1432 and 1613 $cm^{-1}$; these can be assigned to the symmetric and asymmetric O-C-O vibrations, respectively, which confirms the findings from FTIR. Similar energy shifts of the O-C-O vibrations between the FTIR and the Raman measurements of terephthalate anions have also been reported by Lee et al.[58] Here, it is important to remember that the assignments to vibrations of functional groups are simplifications as these vibrations are always coupled to the rest of the molecule. The signal of 861 $cm^{-1}$ is a C-C stretching of the carboxyl group and that at 1137 $cm^{-1}$ a superposition of breathing of the aromatic ring and C-H in-plane bending.[59]

Finally, to address the oxidation state of copper in our hybrid thin films, we collected XPS spectra for the Cu-TPA, Cu-ODA and Cu-PPDA thin films, see Fig. 6(a). First of all, the Cu 2p regions are clearly different for the Cu-PPDA and Cu-TPA films, which can be interpreted

such that Cu is mainly in the oxidation states +I and +II in these two films, respectively. The $2p_{3/2}$ and $2p_{1/2}$ peaks shift to higher binding energies for the Cu(II) compound, namely from 932.3 to 934.8 eV and from 952.1 to 954.7 eV, respectively. Furthermore, the Cu-TPA film has strong shoulder peaks between 938.4 and 946.4 eV and at 963.1 eV as expected for Cu(II). The Cu LMM Auger transitions for the three films are shown in the inset of Fig. 6(a). The values of 571. 6 and 571.0 eV also indicate Cu(II) for the Cu-TPA film and Cu(I) for the Cu-PPDA film. A reduction of copper to the oxidation state +I in $Cu(dmap)_2$ has also reported for thermal ALD processes with $H_2O$ yielding $Cu_2O$[46] and with $NH_3$ yielding $Cu_3N$.[47] The XPS data for the Cu-ODA film are the most difficult to interpret, but comparing the Cu 2p and Cu LMM features with those seen for Cu-TPA and Cu-PPDA, it seems likely that both Cu(I) and Cu(II) exist in Cu-ODA.

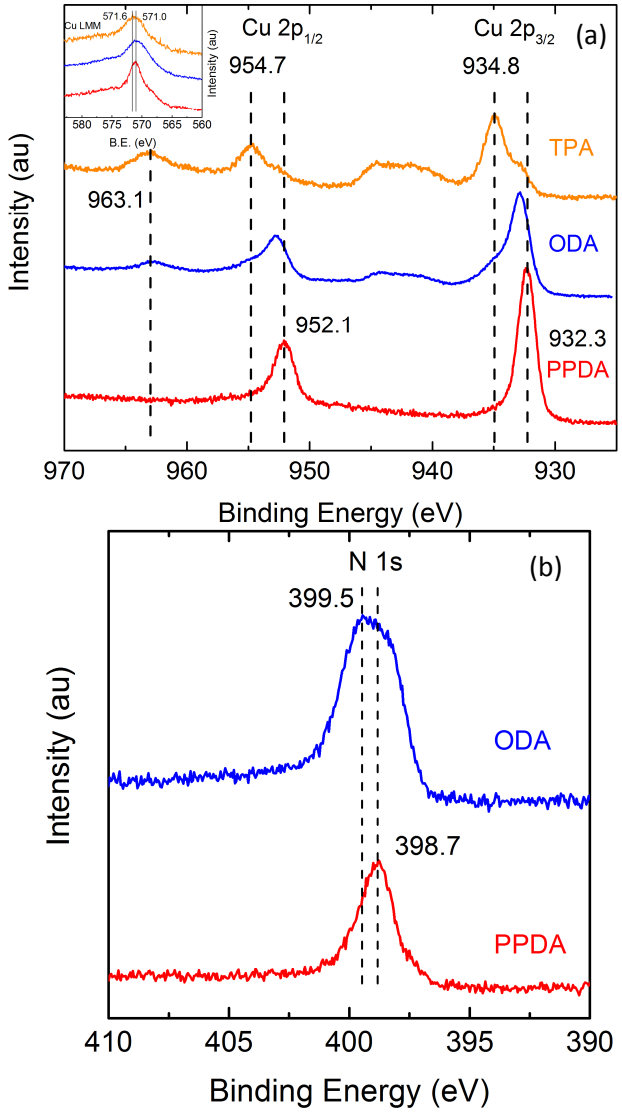


**Fig. 6** XPS spectra of Cu-organic films deposited with $Cu(dmap)_2$: (a) Cu 2p region of Cu-TPA, Cu-ODA and Cu-PPDA, the insert shows the Cu LMM Auger peak, (b) N 1s region of Cu-ODA and Cu-PPDA.

The nitrogen 1s spectra for the same Cu-ODA and Cu-PPDA films are shown in Fig. 6(b). The Cu-PPDA film is dominated by a feature at 398.7 eV, which is consistent with the presence of imino groups.[60] The N 1s Si of the Cu-ODA film on the other hand consists of two components, one at 399.5 eV and one at 398.7. This can be interpreted as originating from the coexistence of amino and imino groups. In the FTIR and Raman spectra of the Cu-ODA film in Fig. 5, small features exist that might originate from imino groups. However, the measuring of the XPS spectra of the Cu-organic films was problematic due to the tendency of the Cu(II) cations to get reduced by X-ray radiation. Furthermore, a damage of the film structure by sputtering was observed which limited the analysis to the surface which was exposed to atmosphere during a fast transfer to the XPS instrument. Nevertheless, the differences in the reaction mechanisms of the quite similar molecules ODA and PPDA with $Cu(dmap)_2$ could be confirmed.

To conclude our studies for the reaction schemes and resultant bonding structures, we present schematically in Fig. 7 possible structures for our Cu-organic hybrid thin films obtained from the six different ALD/MLD processes investigated. The reactions of $Cu(dmap)_2$ with TPA, BDT and HQ (at low deposition temperatures) appeared to be simple ligand exchange reactions. In these reactions a proton is transferred from the functional group of the organic precursor to the dmap anion and the organic molecule binds to the Cu cation. This was confirmed by FTIR as a presence of all the signals expected for the aromatic ring and the decline of the signals expected for the functional groups. Additionally, for Cu-TPA vibrations associated with anionic carboxyl groups were seen, and the FTIR data moreover indicated that the carboxyl groups are bound to copper in a bridging configuration. The bulk form of Cu-TPA crystallises in a paddle-wheel MOF structure,[61,62] and crystalline Cu-TPA films of this structure were obtained in our previous work from $Cu(acac)_2$ precursor.[18] Although only amorphous films were obtained in this work the FTIR and Raman data are consistent with this structure.

Our observations for Cu-PPDA were quite different, since the FTIR features associated with the aromatic ring were extremely weak and both FTIR and Raman suggested the presence of a quinoid-type ring -N=$C_6H_4$=N-, and also a Stokes line consistent with an imino group was identified. One explanation is a secondary reaction converting a primary phenylen-diamide into a quinone-diimide: R-Cu-NH-$C_6H_4$-NH-Cu-R → R-Cu-N=$C_6H_4$=N-Cu-R + 2H. The structure of Cu-ODA was the most difficult to interpret. While the FTIR spectra showed that the aromatic rings and amino groups of most organic moieties were present after the reaction, the existence of imino groups could not be ruled out. Furthermore, the XPS investigation revealed that both Cu(I) and Cu(II) are present. However, combining the data we conclude that Cu(II) bound to deprotonated amino groups is the dominant species.

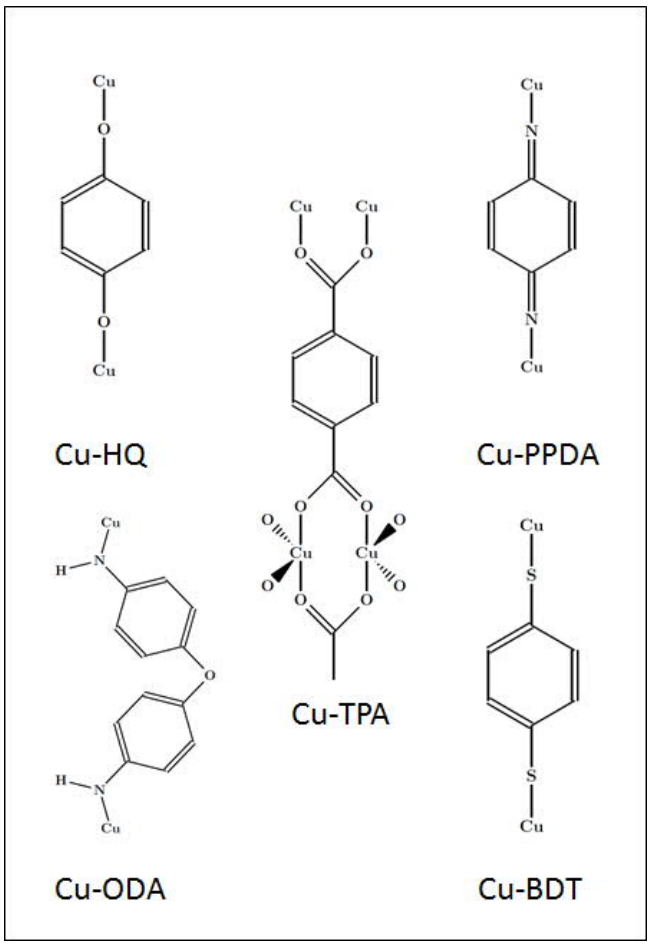


**Fig. 7** Possible structures of Cu-hybrids discussed in this work.

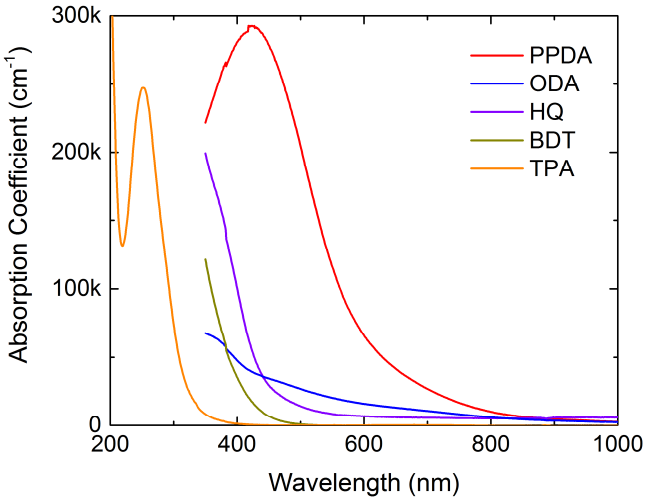


**Fig. 8** UV-vis-NIR spectra for the six different Cu-organic hybrid thin films. For these measurements, Cu-TPA was deposited on quartz glass, the others on borosilicate glass.

**Photoabsorption characteristics.** The coordination sphere about the Cu cation was anticipated to have a significant effect on the optical properties of our Cu-organic films. Therefore, we measured the UV-vis absorption spectra for the films. From Fig. 8, the absorption spectra indeed strongly depend on the organic component. The Cu-TPA film is transparent throughout the visible region and absorbs strongly in the near UV, where the $\pi$-$\pi^*$ adsorption edge of the aromatic ring is expected. This is consistent with the planar coordination of $Cu^{2+}$ ions in the paddle-wheel structure suggested here for our Cu-TPA films since the essentially quadratic coordination typically leads to a large ligand field splitting. The spectrum for Cu-PPDA can be regarded as the opposite extreme, as it reveals strong absorption throughout the visible region. Also Cu-ODA absorbs throughout the visible region; however, compared to Cu-PPDA, the absorption is much weaker. For Cu-HQ, the main absorption step is around 450 nm, but another significant absorption peak is seen in the lower energy side. Finally, for Cu-BDT the main absorption feature is shifted – compared to that of Cu-HQ – to slightly lower wavelengths, suggesting a stronger ligand field for the former.

## Conclusions

Five different aromatic organic precursors were investigated in combination with the aminoalkoxide $Cu(dmap)_2$ as the transition metal precursor in ALD/MLD processes for the fabrication of hybrid Cu-organic thin films. All the six new processes yielded amorphous hybrid films with growth rates that are typical for a majority of the ALD/MLD processes. The processes with ODA and PPDA were investigated in more detail, and saturated growth was achieved with both precursors within a considerably wide temperature window with an upper limit at about 200 °C set by the onset of the decomposition of $Cu(dmap)_2$ and the lower limit determined by the sublimation temperatures of 140 °C for ODA and 70 °C for PPDA.

For hybrid Cu-organic thin films, only one ALD/MLD process was known prior to the present work, i.e. the $Cu(thd)_2$+TPA process which yielded crystalline Cu-TPA thin films within the narrow temperature range of 180–190 °C, otherwise amorphous hybrid films at the higher deposition temperatures.[18] Here, we found that, even though the use of $Cu(dmap)_2$ as the copper precursor allowed the depositions at the lower temperature of 160 °C, the $Cu(dmap)_2$+TPA process resulted in amorphous hybrid films within the entire deposition temperature range investigated. Otherwise, the two processes however behaved in an essentially similar manner, including the growth rates achieved. It should also be noted that the bonding characteristics were found to be very similar in both the amorphous and crystalline Cu-TPA films, independent of the copper precursor employed.

Then, comparing the $Cu(dmap)_2$+HQ process developed here with the similar process where $Cu(acac)_2$ was used as the copper precursor, it was found that while the $Cu(acac)_2$+HQ process yielded metallic Cu films thorough a wide deposition temperature range,[51] the $Cu(dmap)_2$+HQ process is temperature dependent such that it results in metallic Cu films only at the higher deposition temperatures; at temperatures below 120 °C the process successfully yielded hybrid Cu-HQ films. Also importantly, the as-deposited amorphous hybrid films were strongly air and moisture sensitive and crystallised upon the reaction with water. The diffraction pattern did not match to any known Cu-organic material, indicating towards a new crystalline hybrid phase.

Apparently, copper in the $Cu(dmap)_2$ precursor may also be reduced to the monovalent state upon the reaction with an

organic precursor. This was shown – on the bases of XPS analysis – to be the case at least in the $Cu(dmap)_2$+PPDA process.

Despite the possibly somewhat sluggish reactivity of amino groups with $Cu(dmap)_2$, the diamine PPDA precursor was found to readily react with $Cu(dmap)_2$ resulting in well-defined Cu-organic hybrid films within the entire deposition temperature investigated. An interesting feature with this process is that the FTIR and Raman analysis indicated towards a secondary reaction yielding Cu-organic films with iminoquinone-type moieties.

Finally, the $Cu(dmap)_2$+BDT process developed in this work is the first demonstration of the use of the benzene dithiol as the organic precursor in ALD/MLD; the attractive feature of BDT is its low evaporation temperature which allowed – when combined with the readily evaporated $Cu(dmap)_2$ precursor – the hybrid Cu-BDT film depositions to be carried out at ultra-low temperatures down to 80 °C.

## Acknowledgements

This work has received funding from the European Research Council under the European Union's Seventh Framework Programme (FP/2007-2013)/ERC Advanced Grant Agreement (No. 339478), and the Academy of Finland (No. 296299). We acknowledge the provision of facilities and technical support by Aalto University at OtaNano - Nanomicroscopy Center (Aalto-NMC).

## References

[1] C. Sanchez, C. Boissiere, S. Cassaignon, C. Chaneac, O. Durupthy, M. Faustini, D. Grosso, C. Laberty-Robert, L. Nicole, D. Portehault, F. Ribot, L. Rozes, and C. Sassoye, *Chem. Mater.*, 2014, **26**, 221 – 238.
[2] I. Stassen, N. Burtch, A. Talin, P. Falcaro, M. Allendorf, and R. Ameloot, *Chem. Soc. Rev.*, 2017, **46**, 3185–3241.
[3] O. Nilsen, K. Klepper, H. Nielsen, and H. Fjellvåg, *ECS Trans.*, 2008, **16**, 3 – 14.
[4] A. A. Dameron, D. Seghete, B. B. Burton, S. D. Davidson, A. S. Cavanagh, J. A. Bertrand, and S. M. George, *Chem. Mater.*, 2008, **20**, 3315 – 3326.
[5] P. Sundberg and M. Karppinen, *Beilstein J. Nanotech.*, 2014, **5**, 1104 – 1136.
[6] S. M. George, *Chem. Rev.*, 2010, **110**, 111–131.
[7] H.-I. Shao, S. Umemoto, T. Kikutani, and N. Okui, *Polymer*, 1997, **38**, 459 – 462.
[8] M. Vähä-Nissi, P. Sundberg, E. Kauppi, T. Hirvikorpi, J. Sievänen, A. Sood, M. Karppinen, and A. Harlin, *Thin Solid Films*, 2012, **520**, 6780 – 6785.
[9] C. Hossbach, F. Nehm, A. Singh, H. Klumbies, D. Fischer, C. Richter, U. Schroeder, M. Albert, L. Müller-Meskamp, K. Leo, T. Mikolajick, and J. W. Bartha, *J. Vac. Sci. Tech. A*, 2014, **33**, 01A119.
[10] J.-P. Niemelä and M. Karppinen, *Dalton Trans.*, 2014, **44**, 591–597.
[11] Z. Giedraityte, P. Sundberg, and M. Karppinen, *J. Mater. Chem. C*, 2015, **3**, 12316 – 12321.
[12] Z. Giedraityte, L.-S. Johansson, and M. Karppinen, *RSC Advances*, 2016, **6**, 103412 – 103417.
[13] Z. Giedraityte, J. Sainio, D. Hagen, and M. Karppinen, *J. Phys. Chem. C*, 2017, **121**, 17538 – 17545.
[14] Z. Giedraityte, M. Tuomisto, M. Lastusaari, and M. Karppinen, *ACS Appl. Mater. Interfaces*, 2018, **10**, 8845 – 8852.
[15] A. Räupke, F. Albrecht, J. Maibach, A. Behrendt, A. Polywka, R. Heiderhoff, J. Helzel, T. Rabe, H.-H. Johannes, W. Kowalsky, E. Mankel, T. Mayer, P. Görrn, and T. Riedl, *ECS Trans.*, 2014, **64**, 97–105.
[16] T. Tynell, I. Terasaki, H. Yamauchi, and M. Karppinen, *J. Mater. Chem. A*, 2013, **1**, 13619 – 13624.
[17] T. Tynell, A. Giri, J. Gaskins, P. E. Hopkins, P. Mele, K. Miyazaki, and M. Karppinen, *J. Mater. Chem. A*, 2014, **2**, 12150 – 12152.
[18] E. Ahvenniemi and M. Karppinen, *Chem. Commun.*, 2016, **52**, 1139 – 1142.
[19] E. Ahvenniemi and M. Karppinen, *Chem. Mater.*, 2016, **28**, 6260 – 6265.
[20] M. Nisula, J. Linnera, A. J. Karttunen, and M. Karppinen, *Chem. Eur. J.*, 2017, **23**, 2988 – 2992.
[21] J. Penttinen, M. Nisula, and M. Karppinen, *Chem Eur. J.*, 2017, **23**, 18225 –18231.
[22] K. V. d. Kerckhove, F. Mattelaer, J. Dendooven, and C. Detavernier, *Dalton Trans.*, 2017, **46**, 4542 – 4553.
[23] K. V. d. Kerckhove, F. Mattelaer, D. Deduytsche, P. M. Vereecken, J. Dendooven, and C. Detavernier, *Dalton Trans.*, 2016, **45**, 1176 – 1184.
[24] C. Ban and S. M. George, *Adv. Mater. Interfaces*, 2016, **3**, 1600762.
[25] Q. Peng, B. Gong, R. M. VanGundy, and G. N. Parsons, *Chem. Mater.*, 2009, **21**, 820 – 830.
[26] N. M. Adamczyk, A. A. Dameron, and S. M. George, *Langmuir*, 2008, **24**, 2081–2089.
[27] B. Yoon, Y. Lee, A. Derk, C. Musgrave, and S. George, *ECS Trans.*, 2011, **33**, 191 – 195.
[28] A. Sood, P. Sundberg, J. Malm, and M. Karppinen, *Appl. Surf. Sci.*, 2011, **257**, 6435 – 6439.
[29] A. Sood, P. Sundberg, and M. Karppinen, *Dalton Trans.*, 2013, **42**, 3869 – 3875.
[30] P. Sundberg and M. Karppinen, *Europ. J. Inorg. Chem.*, 2014, **2014**, 968–974.
[31] E. Ahvenniemi, M. Matvejeff, and M. Karppinen, *Dalton Trans.*, 2015, **44**, 8001–8006.
[32] K. Uusi-Esko, E.-L. Rautama, M. Laitinen, T. Sajavaara, and M. Karppinen, *Chem. Mater.*, 2010, **22**, 6297 – 6300.
[33] K. Uusi-Esko and M. Karppinen, *Chem. Mater.*, 2011, **23**, 1835 – 1840.
[34] E. Ahvenniemi and M. Karppinen, *Dalton Trans.*, 2016, **45**, 10730 – 10735.
[35] M. Nisula and M. Karppinen, *Nano Lett.*, 2016, **16**, 1276 – 1281.
[36] L. C. Kalutarage, S. B. Clendenning, and C. H. Winter, *Chem. Mater.*, 2014, **26**, 3731 – 3738.
[37] L. C. Kalutarage, P. D. Martin, M. J. Heeg, and C. H. Winter, *J. Am. Chem. Soc.*, 2013, **135**, 12588 – 12591.
[38] L. C. Kalutarage, P. D. Martin, M. J. Heeg, and C. H. Winter, *Inorg. Chem.*, 2013, **52**, 5385–5394.
[39] J. P. Klesko, M. M. Kerrigan, and C. H. Winter, *Chem. Mater.*, 2016, **28**, 700 – 703.
[40] T. J. Knisley, T. C. Ariyasena, T. Sajavaara, M. J. Saly, and C. H. Winter, *Chem. Mater.*, 2011, **23**, 4417 – 4419.
[41] J. P. Coyle, G. Dey, E. R. Sirianni, M. L. Kemell, G. P. A. Yap, M. Ritala, M. Leskelä, S. D. Elliott, and S. T. Barry, *Chem. Mater.*, 2013, **25**, 1232 – 1238.

 

[42] D. J. Hagen, I. M. Povey, S. Rushworth, J. S. Wrench, L. Keeney, M. Schmidt, N. Petkov, S. T. Barry, J. P. Coyle, and M. E. Pemble, *J. Chem. Mater. C*, 2014, **2**, 9205 – 9214.
[43] D. Hagen, J. Connolly, R. Nagle, I. Povey, S. Rushworth, P. Carolan, P.Ma, and M. Pemble, *Surf. Coat. Tech.*, 2013, **230**, 3–12.
[44] B. H. Lee, J. K. Hwang, J. W. Nam, S. U. Lee, J. T. Kim, S.-M. Koo, A. Baunemann, R. A. Fischer, and M. M. Sung, *Angew. Chem. Int. Edit.*, 2009, **121**, 4606–4609.
[45] K. Väyrynen, K. Mizohata, J. Räisänen, D. Peeters, A. Devi, M. Ritala, and M. Leskelä, *Chem. Mater.*, 2017, **29**, 6502 – 6510.
[46] J. R. Avila, A. W. Peters, Z. Li, M. A. Ortuño, A. B. F. Martinson, C. J. Cramer, J. T. Hupp, and O. K. Farha, *Dalton Trans.*, 2017, **46**, 5790 – 5795.
[47] J.-M. Park, K. Jin, B. Han, M. J. Kim, J. Jung, J. J. Kim, and W.-J. Lee, *Thin Solid Films*, 2014, **556**, 434–439.
[48] R. Becker, A. Devi, J. Weiss, U. Weckenmann, M. Winter, C. Kiener, H.-W. Becker, and R. A. Fischer, *Chem. Vapor Depos.*, 2003, **9**, 149–156.
[49] B. Yoon, D. Seghete, A. S. Cavanagh, and S. M. George, *Chem. Mater.*, 2009, **21**, 5365 – 5374.
[50] S. C. Goel, K. S. Kramer, M. Y. Chang, and W. E. Buhro, *Polyhedron*, 1990, **9**, 611 – 614.
[51] T. S. Tripathi and M. Karppinen, *Chem. Mater.*, 2017, **29**, 1230–1235.
[52] T. Tynell and M. Karppinen, *Thin Solid Films*, 2014, **551**, 23–26.
[53] K. B. Klepper, O. Nilsen, P.-A. Hansen, and H. Fjellvåg, *Dalton Trans.*, 2011, **40**, 4636 – 4646.
[54] X.-G. Li, M.-R. Huang, R.-F. Chen, Y. Jin, and Y.-L. Yang, *J. Appl. Polymer Sci.*, 2001, **81**, 3107 – 3116.
[55] T. Ohashi, E. Kobayashi, T. Jinbo, and J. Furukawa, *J. Polymer Sci. A*, 1997, **35**, 1621 – 1625.
[56] S. H. Cho, H. S. Han, D.-J. Jang, K. Kim, and M. S. Kim, *J. Phys. Chem.*, 1995, **99**, 10594 – 10599.
[57] M. Trchová, Z. Morávková, M. Bláha, and J. Stejskal, *Electrochim. Acta*, 2014, **122**, 28–38.
[58] M. W. Lee, M. S. Kim, and K. Kim, *J. Molec. Str.*, 1997, **415**, 93 – 100.
[59] G. Kumari, N. R. Patil, V. S. Bhadram, R. Haldar, S. Bonakala, T. K. Maji, and C. Narayana, *J. Raman Spec.*, 2016, **47**, 149 – 155.
[60] G. Kowalski, J. Pielichowski, and M. Grzesik, *Sci. World J.*, 2014, **2014**, 648949.
[61] C. G. Carson, K. Hardcastle, J. Schwartz, X. Liu, C. Hoffmann, R. A. Gerhardt, and R. Tannenbaum, *Europ. J. Inorg. Chem.*, 2009, **2009**, 2338 – 2343.
[62] R. Adams, C. Carson, J. Ward, R. Tannenbaum, and W. Koros, *Micropoorous Mesoporous Mater.*, 2010, **131**, 13 – 20.